Journal of Materials Chemistry A

ROYAL SOCIETY OF CHEMISTRY

PERSPECTIVE

Cite this: *J. Mater. Chem. A*, 2020, **8**, 513

Solar evaporation for simultaneous steam and power generation

Guohua Liu, [a] Ting Chen,[b] Jinliang Xu,*[a] Gang Li[c] and Kaiying Wang *[cd]

Received 6th November 2019
Accepted 26th November 2019

DOI: 10.1039/c9ta12211g

rsc.li/materials-a

The rapid development of photothermal materials and their integrated systems has fostered recent technology breakthroughs in solar evaporation for both steam and power generation. Here, we discuss this new and emerging area that aims to directly couple photothermal materials and solar steam devices towards clean water and electricity generation. The photothermal conversion physics and engineering strategies of solar absorbers were first described. The electricity generation mechanisms to be covered include triboelectric, pyroelectric, piezoelectric, thermoelectric, thermal-electrochemical and salinity gradient effects. The diverse systems were then systematically scrutinized and discussed towards better harvesting and conversion of solar energy. The operation principles were described and the performance requirements were elaborated together with the advantages and the limitations. Comparisons of the solar evaporation and electric performances were additionally made for such developed systems. Finally, the future research directions of the systems were highlighted, and the potentials for new applications and hybrid approaches in the development of a Synergy City were outlined.

1. Introduction

Water steam plays a vital role in industrial revolution that is mostly known for the steam-driven turbines in power plants.[1,2] By use of mirror arrays, solar steam turbines utilize sunlight on a small volume to produce a high local temperature for water vaporization. The released steam with a high pressure and temperature is then transferred to drive the turbine for electricity generation.[3] In these systems, the solar receiver requires large optical devices, unavoidably suffering from large footprint investments as well as heat losses. Besides, the bulk water also stores a considerable amount of solar energy that is not used in vapor generation.[4] To reduce the cost and improve energy utilization, interfacial solar evaporation is recognized as a potential strategy to meet the future needs (Fig. 1).[5–7] This method uses solar energy more efficiently because the thermal evaporation occurs at the air–water interfaces.[8,9] This interfacial evaporation exhibits a good performance even at an ambient environment, which thus greatly reduces convective and

[a]*Beijing Key Laboratory of Multiphase Flow and Heat Transfer for Low Grade Energy Utilization, North China Electric Power University, Beijing, 102206, China. E-mail: xjl@ncepu.edu.cn*

[b]*School of Chemical and Environmental Engineering, Jianghan University, Wuhan, 430056, China*

[c]*Institute of Energy Innovation, Taiyuan University of Technology, Taiyuan, 030024, China*

[d]*Department of Microsystems, University of South-Eastern Norway, Horten 3184, Norway. E-mail: Kaiying.Wang@usn.no*

Guohua Liu received PhD in Engineering of Thermophysics from Chinese Academy of Sciences in 2010. He obtained his 2nd PhD in Micro and Nano Systems Technology at University of South-Eastern Norway (USN), 2013. Currently, he is a full professor at North China Electric Power University. His research interests center on the development and assembly of nanostructured materials for energy applications.

Ting Chen received her PhD in Materials Physics and Chemistry from Sun Yat-sen University in 2014. Currently, she is working at Jianghan University as a full faculty member. Her research interests are centered on the development of nanostructured materials for energy applications and the design and optimization of chemical engineering processes.

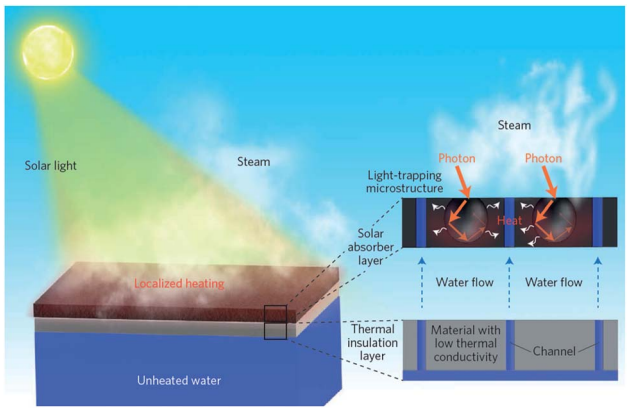

Fig. 1 Interfacial solar evaporation. The photothermal material enables broadband solar absorption and converts photon energy to heat localized at the air–water interfaces. The embedded capillary channels in insulation layer transport the water to the hot evaporative surface for direct steam generation. Reproduced with permission.[6] Copyright 2017 Nature Publishing Group.

radiative heat losses. Moreover, the bulk liquid at an ambient temperature does not consume the absorbed solar energy to heat up water.[10,11] By this facile approach, solar-to-vapor conversion efficiencies above 90% have been recently demonstrated in several studies.[12–14]

Besides storing solar energy as heat in vapor, there exist diverse chances to harvest the waste energy in solar evaporation, *e.g.*, the upward flow brought by solar thermal evaporation, the induced salinity difference and temperature difference around the surrounding environment of the absorber, *etc.*[15–21] The upward flow driven by evaporation has been introduced to produce electricity due to the streaming potential effect, in which the flow is passed through porous aluminum oxide membranes, carbon films or graphene cloths.[22–26] Using an ion selective membrane, the simultaneous production of water steam and electricity has also been realized owing to the induced salinity gradient from evaporation.[27] Due to the localized heating at the air–water interface, the temperature difference from air to the solar absorber and bulk liquid can be quite large. This offers an additional opportunity for power generation with steam releasing from water. A series of technologies such as thermoelectric, pyroelectric and thermogalvanic modules have been introduced to recover the waste heat energy between the solar absorber and the surrounding environment.[28–30] All the studies reflect that the rational combination of solar evaporation with proper electricity technologies is a potential avenue for obtaining both fresh water and power supply.

In this context, we discuss the state-of-the-art developments of interfacial solar evaporation for both clean water and electricity production. Waste energy harvesting mechanisms to be covered in the evaporation process include triboelectric, pyroelectric, piezoelectric, thermoelectric, thermal-electrochemical and salinity gradient effects (Fig. 2). Triboelectric charges are produced as a result of a frictional contact between two materials that become electrically charged.[31] They are typically used as flow energy harvesting devices to harness triboelectric energy induced by the condensate steam. The thermoelectric effect generates charges from a thermal gradient between two dissimilar conductors due to the Seebeck effect[32] and can be typically used as a harvesting device for waste heat recovery. We will see that this mechanism of charge generation can take the form of an external harvesting device that is separated from the solar absorber, or it can take the form of an all-in-one device that is in direct contact with photothermal materials. The pyroelectric, thermal-electrochemical and piezoelectric effects generate an electric charge as a result of a polarization change in materials due to the temperature change or strain gradient,[33–35] while the salinity gradient power arises from novel fluidic transport due to high ionic flux and surface charge density.[36,37] We will see that in some cases, the hybrid mechanism works by more than one of the harvesting approaches. Table 1 provides a summary of the harvesting mechanisms, solar absorber materials, operation modes and applications. We will refer to this table throughout the review. The photothermal physics and engineering strategies of solar materials are briefly presented. The interactions of photothermal materials and solar steam devices with electricity generation systems are then

Jinliang Xu is the Dean of School of Mechanical and Power Engineering, North China Electric Power University, China. His research interest focuses on micro/nano heat transfer, micro energy system, and multiphase flow and heat transfer. He has published more than 100 papers in recognized academic journals. He has served as International conference chair or co-chair for several times in related area.

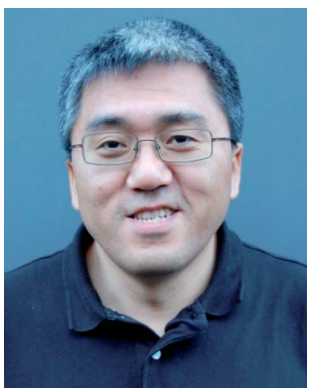

Kaiying Wang received PhD in condensed matter physics from the Institute of Physics, Chinese Academy of Sciences in 1995. He was a postdoc at University of New Orleans, USA. He joined University of South-Eastern Norway (USN) in 2007 as an associate professor and then was promoted as professor in 2010. His research interests focus on micro-fabrication and nano-technology, functional thin films, magnetic and superconductive materials, nanostructure characterization and nanodevices for environment and energy applications.

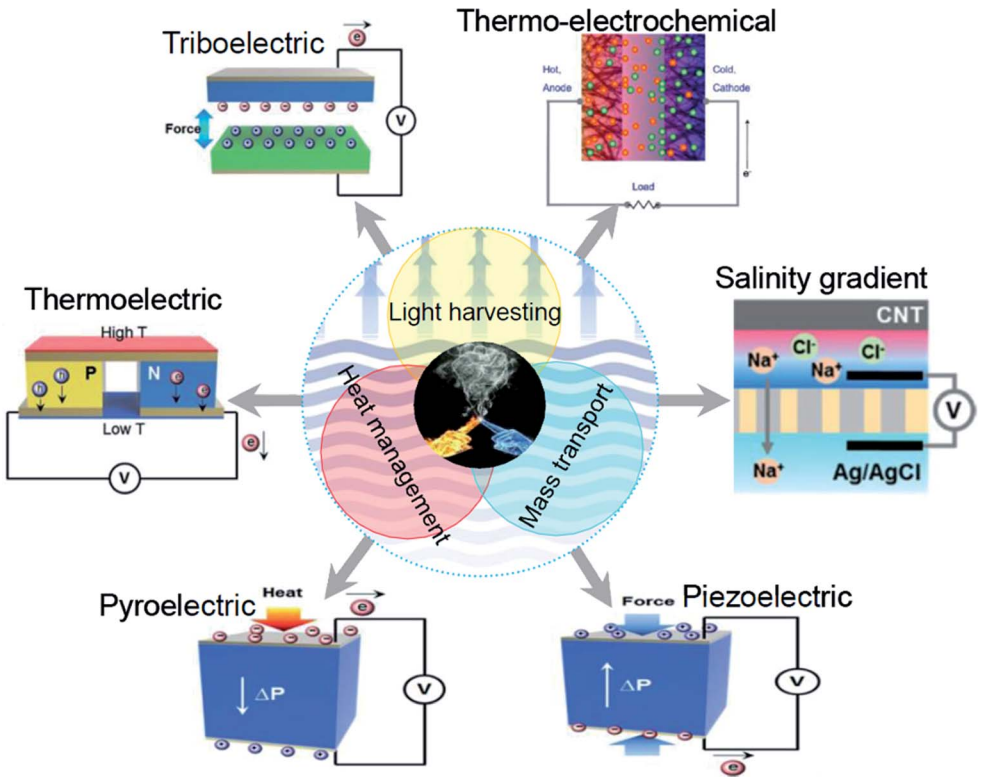

Fig. 2 Triboelectric (motion), pyroelectric (temperature fluctuation), thermoelectric (temperature gradients), piezoelectric (strain), thermo-electrochemical (temperature dependence of redox reaction) and salinity gradient (solar excitation) charge generation mechanisms, which are used to integrate the solar hybrid devices for both clean water and electricity generation.

addressed together with their potential applications. Finally, we point out research opportunities and outline a vision of applications they would enable.

2. Photothermal physics and solar materials engineering

Photothermal conversion is an energy conversion process, where light energy incident on a material is transformed into thermal energy. The photothermal materials are key components to support this conversion since they can absorb incident light and convert it into heat *via* photoexcitation. An ideal material should absorb light over a broad range of solar spectrum to promote thermal energy output. A variety of materials have been demonstrated to show strong light absorption including carbon-based nanomaterials, plasmonic nanomaterials and inorganic semiconductors. These absorbers rely on three kinds of photoexcitations: thermal vibration of molecules, plasmonic heating[38,39] and electron–hole generation and relaxation.[40–42] In this section, we discuss these general physics as well as materials engineering for efficient light-to-heat conversion.

2.1. Thermal vibration in molecules

Carbon-based materials such as amorphous carbon, carbon black and graphite are naturally black and have good ability for solar light harvesting owing to the optical transitions of their π-bands.[9,10] The loosely held electrons in the π orbital are excited and jump from the π orbital to the π* orbital with a small energy input. Besides, the conjugated π-bonds give rise to a red-shift in their absorption spectrum. On increasing the number of π-bonds, the energy bandgap between the highest occupied molecular orbital (HOMO) and the lowest unoccupied molecular orbital (LUMO) decreases (Fig. 3a). The absorption wavelength of these bands depends on the spacing of their electronic levels and thus, a large number of conjugated π-bonds can promote the photo-excitation of electrons over a broad range of the solar spectrum. Heat is then generated when the excited electrons relax to the ground state *via* electron–electron and electron–phonon scattering, resulting in an overall increase in temperature. Therefore, the photothermal effect of carbon-based materials involves the broadband photo-excitation of electrons and their subsequent relaxation and vibrational modes throughout the atomic lattices.[40]

Carbon materials have limited absorptivity by a moderate reflection of 5–10% at the air-dielectric interface.[8,9] Hereby, the materials engineering focuses on reducing light reflection and amplifying light flux. Porous absorbers such as carbon foams,[28] flame-treated or carbonized wood,[43,44] polymeric gel networks,[14] carbon nanotubes (CNTs)/cellulose nanocrystal composite sponges[30] and porous graphite/graphene[45] are promising candidates.[46–48] By these designs, the mesoscale structures partially absorb light as well as reflect and scatter it, and the nanostructured interface induces light rays to bend

Table 1 An up-to-date summary of interfacial solar evaporation for simultaneous steam and power generation

Mechanism	Energy source	System configuration	Solar harvesting material	Substrate	Photothermal conversion	Solar intensity (kW m^{-2})	Solar absorption (%)	Rate (kg m^{-2} h^{-1})	Vaporization efficiency (%)	Voltage (V)	Power density (W m^{-2})	Application	Ref.
Triboelectric	Mechanical	All-in-one	Au nanoflowers	Porous silica matrix	Plasmonic heating	1 sun	>70%, 00–1200 nm	1.356	85	~3.0	890 × 10^{-6}	Distillation	71
Piezo-pyroelectric	Mechanical-thermal	Separation	Nitrogenenriched carbon sponge	Carbon sponge	Thermal vibration	1 sun	>95% full wavelength	1.39	90	−20	240.7 × 10^{-6}	Electricity and fresh water	28
Thermoelectric	Thermal	Separation	Graphite	Nonwoven film	Thermal vibration	8–30 sun	~98%, 250–2500 nm	4.2–34.8	72.2	4.15	0.9–292.9	Storing steam enthalpy	45
Thermoelectric	Thermal	All-in-one	Carbonaceous materials	Sponge	Thermal vibration	1 sun	~95%, 250–2500 nm	1.26	81	0.095	0.4	Food waste utilization	92
Thermoelectric	Thermal	All-in-one	Carbon nanotubes/cellulose nanocrystals	Polydimethylsiloxane sponge	Thermal vibration	1 sun	>93% visible and near infrared spectra	1.36	87.4	0.06–0.263	6.73	Electricity and water	30
Thermo-electrochemical	Thermal-chemical	All-in-one	Graphite film	Graphite film	Thermal vibration	1 sun	>90%, 250–2500 nm	1.10	61	0.2	0.0005	Electricity and clean water	29
Salinity	Chemical	All-in-one	Carbon nanotube	Filter paper	Thermal vibration	0.1–2 sun	>90%, 300–2000 nm	2.25	75	0.108	1.1	Fresh water and energy	27

progressively when the light wavelength is larger than the structure dimension.[49] Moreover, when the geometrical constraints are applied to the spacing and depth among nanostructures in the textured surfaces, light rays can be trapped in the micro/nano-scale gaps and absorbed by multiple internal reflections.[50] As a result, maximum absorption of the incident light can be achieved for converting the incident radiation into useful heat. For example, CNTs can be prepared into porous membranes with controlled thicknesses and pore sizes by filtration and spin-coating methods (Fig. 3b). Vertically aligned CNTs exhibit a constant emissivity of 0.98–0.99 over a spectral range of 0.2–200 μm.[46] Hierarchical graphene foams tuned with continuous porosity *via* plasma-enhanced chemical vapor deposition show great enhancement in the omnidirectional absorption of sunlight, thereby enabling solar-to-vapor efficiency above 90%.[48]

2.2. Plasmonic heating

Plasmonic metals such as gold, silver and platinum can produce intense heat under solar irradiation due to their unique optical characteristics, stemming from the surface plasmon resonance (SPR) effect.[9,38,51] When the oscillation frequency of the delocalized electrons in a plasmonic metal matches the wave frequency of the incident light, collective excitation of carriers is initiated above the Fermi level to higher energy levels, creating hot electrons to form hot electron clouds (Fig. 3c). These hot electrons are non-radiatively damped and decayed *via* the Landau damping mechanism and redistribute their energy through an electron–electron process, resulting in heat production by a Joule mechanism and rapidly increasing the surface temperature of the metals[38,52] The hot electrons also cool fast by electron–phonon scattering within the metal lattice in picoseconds. The optical skin depth of carrier absorption is about tens of nanometers when the thermal wave propagates at the surface plane. The resulting heat is then dissipated into the surrounding environment through phonon–phonon relaxation at different temporal and spatial scales.[8,9] Therefore, plasmonic metals show strong heat generation *via* surface plasmon resonances since they have many mobile electrons for thermal conversion.

Despite the distinct advantages, plasmonic materials have a fundamental limitation because of their narrow band of light absorption around their resonance peak. The light absorption by plasmonic nanostructures and the associated temperature increase are very sensitive to the shape and composition of the structure (Fig. 3d). Significant efforts have been put into synthesizing novel nanostructures for optimized interactions with the incident light to extend the absorption spectrum. Commonly used strategies include shape or morphology engineering, dielectric surrounding modulation and particle assembly with tunable gaps.[53–55] The SPR peak can be easily tailored by controlling the geometry of metal structures, but the size or shape effect on extending the absorption spectrum is quite limited due to the intrinsic material properties.[56] Hollow nanostructures or geometry asymmetry can extend the absorption band, while dielectric modulation induces a red-shift in the

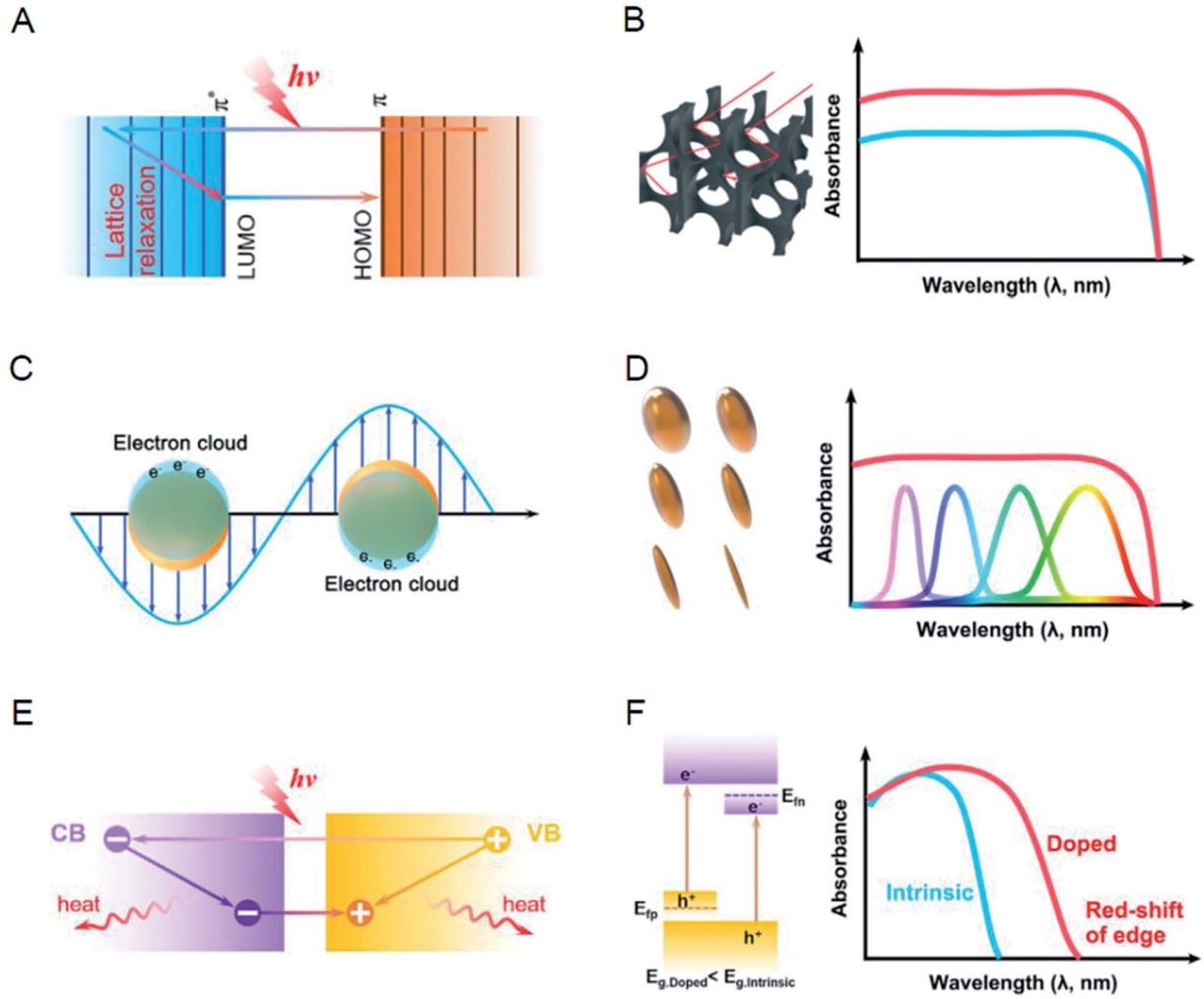

Fig. 3 Photothermal physics and materials engineering with different matters in the corresponding light-absorption range. (A) Thermal vibration of molecules and (B) microstructural engineering, (C) plasmonic heating and (D) geometry and size tuning of particles, (E) photoexcitation and relaxation of charge carriers, (F) band structure engineering. Reproduced with permission.[10,69] Copyright 2019 Elsevier. Copyright 2018 Royal Society of Chemistry.

SPR band, which can be possibly tuned across the optical spectrum into the near-infrared region.[57–59] More importantly, the delicate arrangement or assembly of plasmonic nanoparticles extends the absorption spectral range and red-shifts the peak at the same time.[60,61] For example, owing to the high density optical modes initiated by the multiple scattering effect, a pronounced broadband absorption has been observed in a pore array with close-packed aluminum particles.[62]

2.3. Non-radiative relaxation

Inorganic semiconductor materials have been extensively studied as new kinds of photothermal agents owing to their good biocompatibility and low cytotoxicity.[42,63] The optical absorption spectrum of such materials depends on their bandgap energy. When the photon energy of the incident light is larger than that of the semiconductor bandgap, photo-excited carriers would be generated. The above-bandgap electron–hole pairs are thus produced since most photons from solar irradiation have a high energy above the bandgap. These above-band electrons and holes would eventually restore to the ground states. The damping energy created in the process is finally released to the material *via* either non-radiative relaxation of phonons or radiative relaxation of photons.[8,9] The phonon-type release of energy causes the local heating of the material lattice, leading to an overall temperature increase of the semiconductor (Fig. 3e). Therefore, this temperature distribution and rise are caused due to the diffusion and surface/bulk recombination of photoexcited carriers.[41,64] This mechanism is much different from that in a wideband semiconductor, where most of the absorbed energy is released as photon energy after carrier recombination, resulting in relatively low light-to-heat conversion efficiency.[42]

Semiconductors normally have poor absorption ability in the IR region (700–2500 nm) due to their wide bandgaps. This drawback critically limits their photothermal performance because the IR region occupies ~50% of the total energy of sunlight. Thus, the materials should shift the absorption

spectrum to the near-infrared region. Much attention has been paid to improve the limited absorption *via* tuning their energy bandgap by doping, *e.g.*, introducing impurities or disordered lattices into the materials.[65] Semiconductor doping can tune their electronic band structure in different ways as follows: (1) creating local intra-band energy states *via* the engineering of oxygen vacancies to extend the absorption tails; for example, the oxygen vacancies in titanium dioxide have been demonstrated as an effective way to extend the photo-response of materials from the UV to IR region.[63] (2) Bandgap narrowing of the intrinsic material *via* shifting the conduction or valence position to red-shift the absorption edge (Fig. 3f); for example, the narrowing of the bandgap of Ti_2O_3 results in an absorption spectrum ranging from 500 to 2500 nm of the solar spectrum.[42] (3) Introducing new impurity bands *via* degenerately doping to enlarge the light absorption spectrum. This effect has been verified in degenerately doped semiconductors using a local SPR effect, in which the increase in doping concentration induces a blue-shift in the SPR band.[9,41,64] Moreover, doping also benefits photothermal conversion owing to improved recombination over the materials with more free carriers. So far, black titania and silicon,[63,66] Ti_2O_3 nanoparticles,[42] Cu_7S_4 (ref. 64) and other magnetic bi- or tri-metal oxides[67,68] have been validated as effective photothermal semiconductors for solar evaporation.

3. Solar hybrid systems for simultaneous steam and power generation

Water and energy are precious resources closely related to social development. Solar evaporation is a potential route to meet both necessities.[69,70] Generally, solar evaporation offers a sustainable solution to produce clean water *via* the purification or desalination process. On the other hand, this method also provides great opportunities in evaporation-driven power generation. Up to now, interfacial solar evaporation coupled with a triboelectric,[71] pyroelectric/piezoelectric,[28] thermoelectric,[30,45] thermo-electrochemical or salinity power device[27,29] has been developed for both steam and power generation by the use of free solar energy. With the dual functions in a solar hybrid system at the same time, the overall efficiency of energy conversion can be improved by the rational coupling of solar vaporization with the electricity technologies.

3.1. Triboelectric system

A triboelectric nanogenerator is a kind of mechanical energy harvesting device using the electrification or electrostatic effect.[31,72] In contact electrification, two materials are contacted with each other through friction, which steers the charge transfer between the materials, resulting in triboelectric charging of materials. On the other hand, periodic contact and separation break the distribution of the electrostatic charges on the materials, which induces a potential difference to drive the free electrons to flow. The contact electrification offers static triboelectric charges, and the electrostatic induction effect is responsible for transforming mechanical energy into electricity.[73] The created potential V can be written in the form of $V = \rho d/\varepsilon_0$, in which ρ is the density of triboelectric charges, and ε_0 and d are the vacuum permittivity and gap distance between layers, respectively. The corresponding current flowing through the external circuit is defined as $I = V\frac{\partial C}{\partial t} + C\frac{\partial V}{\partial t}$, where C is the system capacitance and V is the induced potential between electrodes.[74,75] The first term represents the capacitance change in the system induced by mechanical deformation. The second term denotes the potential change coming from contact electrification. A triboelectric nanogenerator has the advantages of flexible material choices and device integration as well as excellent power output, stability and robustness. These advantages enable its new opportunities in water-energy nexus, such as harvesting energy from flowing water,[17] rain droplets,[76,77] water vapor,[22,78] and ocean waves.[79]

A solar hybrid device was recently developed for simultaneous condensate water collection and triboelectricity generation. The solar absorber was made from an inexpensive gel consisting of dispersed gold nanoflowers (AuFs) in a silica matrix (Fig. 4a and b).[71] The intense tip-plasmonic enhancement of AuFs contributed to broadband solar absorption and high-performance photothermal conversion (Fig. 4c). The silica gel also functioned as thermal insulation to confine the plasmonic heat to the small volume of water within the porous matrix, leading to vaporization efficiency of 85% under one sun (Fig. 4d). An overall hybrid device with polytetrafluoroethylene (PTFE) triboelectric energy harvesting materials is shown in Fig. 4e and g. The enclosed space allows vapor condensate flowing along the wall, which produces currents and potential signals due to the flow-induced electrification (Fig. 4h and i). The condensate water is then collected at the vessel bottom (Fig. 4f). The round-bottom design of the vessel (Fig. 4j) can swing the condensate in various directions for harnessing omnidirectional triboelectric energy (Fig. 4k and l). In this way, both the swing movement and the gravitational flow are used to drive energy harvesting. The distinguished advantage of this coupling grants simultaneous clean water production and power generation without stressing on the environment.

3.2. Piezo-pyroelectric system

Stress mechanical energy can be transformed into electricity *via* the piezoelectric effect, which is a coupling state resulting from the mechanical and electrical properties of a material.[34] The material structure would deform after exerting mechanical strain, which drives the charge transport in the material. The density of the polarized charges created by the applied stress is described as $\rho = dX$, where ρ denotes the charge density of polarization, d is the piezoelectric coefficient, and X represents the applied strain. This charge density produces an electric field, which can be given by $\nabla E = \rho/\varepsilon$; here, E and ε are the electric field and the permittivity, respectively.[75,80] The total mechanism of pyroelectricity can be understood from the primary and secondary effects.[33] The primary charge generation comes from the polarization change *versus* temperature change, while the thermal expansion of the material contributes to the

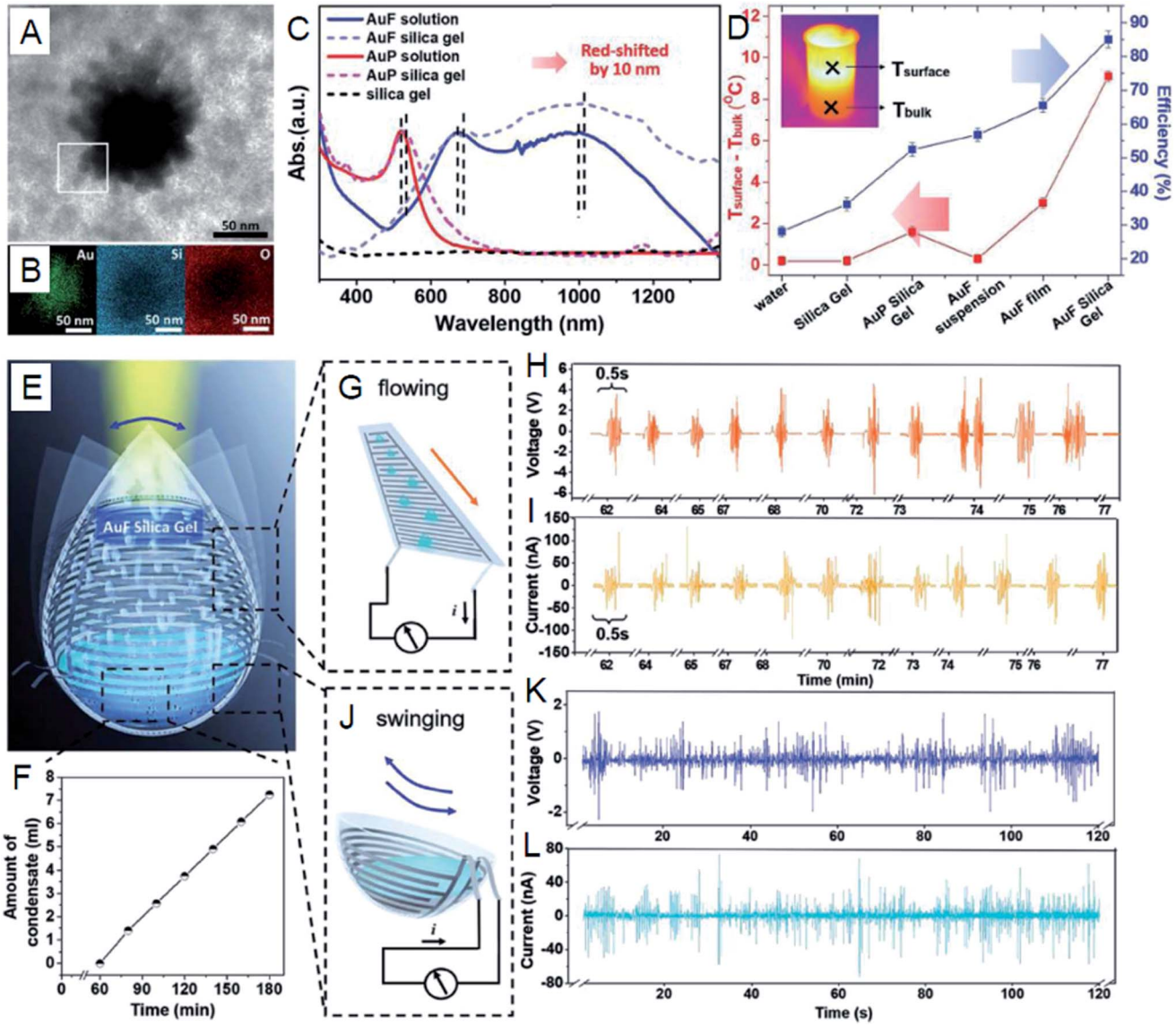

Fig. 4 (A) TEM and (B) EDX characterization of the plasmonic silica gel. (C) The absorption spectra of different samples. (D) The solar-to-steam efficiencies and the resulting temperature differences between the absorber surface and bulk liquid. (E) The solar hybrid device for clean water and triboelectricity. (F) Mass changes of the water condensate. (G) The triboelectric generator for sliding droplets. (H) The created electric potential and (I) current. (J) The triboelectricity from water swinging. (K and L) The electric signal measurement. Reproduced with permission.[71] Copyright 2018 Wiley-VCH.

secondary pyroelectric effect. The corresponding electrical current is defined as $I = \frac{dQ}{dt} = \mu e A \frac{dT}{dt}$, in which Q denotes the resulting charge, μ is the absorption coefficient, A represents the surface area, $\frac{dT}{dt}$ is the temperature variation and e is the pyroelectric coefficient that can be expressed as $e = \frac{d\rho}{dT}$.[81,82] Therefore, the overall polarization can be changed when a pyroelectric material is heated or cooled, leading to a flow current.

A hybrid device not only working as a piezoelectric harvester in a vapor flow, but also functioning as a pyroelectric harvester for temperature fluctuations is desirable to scavenge the lost energy in solar evaporation. For this purpose, a carbon sponge (Fig. 5a) with wideband solar absorption and heat localization properties was designed for *in situ* photothermic vaporization.[28] It was found that the sample with a small pore size of ~25 μm has the best evaporation rate of 1.30 kg m^{-2} h^{-1} (Fig. 5b), with a solar-to-vapor conversion efficiency of 85%. This rate outperformed those of other carbon sponges with large pores and was about 3 times over that of base water. The thermo-mechanical energy from steam turbulence could be harvested by a PVDF tweezer due to its outstanding piezo-pyroelectric properties (Fig. 5c).[83,84] The temperature oscillation and upflow fluctuation could jointly drive the tweezer to produce electricity (Fig. 5d–f). The created electrical current and open-circuit potential could reach −0.08 μA and −20.0 V,

respectively. This combination to convert mechanical friction and temperature change into electricity offers a new concept to simultaneously produce freshwater and electricity. Moreover, the facile synthesis process makes the sponge absorber highly desirable for practical solar-thermal applications.

3.3. Thermoelectric system

Unlike pyroelectric materials requiring a temperature variation *versus* time, thermoelectric devices can generate electrical energy from spatial thermal gradients according to the Seebeck effect. The device efficiency is decided by its operation temperature T and the materials' figure of merit ZT:[85,86] $\eta_{te} = \frac{T_h - T_c}{T_h} \frac{\sqrt{1+ZT}-1}{\sqrt{1+ZT}+\frac{T_c}{T_h}}$ here, ZT is defined as $\frac{\sigma\alpha^2 T}{k_e + k_l}$, σ denotes the electric conductivity, α is the Seebeck coefficient, T_c and T_h are the cold- and hot-side temperatures, respectively, and k is the heat conductivity.[75] There is intense interest to improve the figure of merit for industrial applications. The most common material used so far is Bi_2Te_3.[87,88] Converting

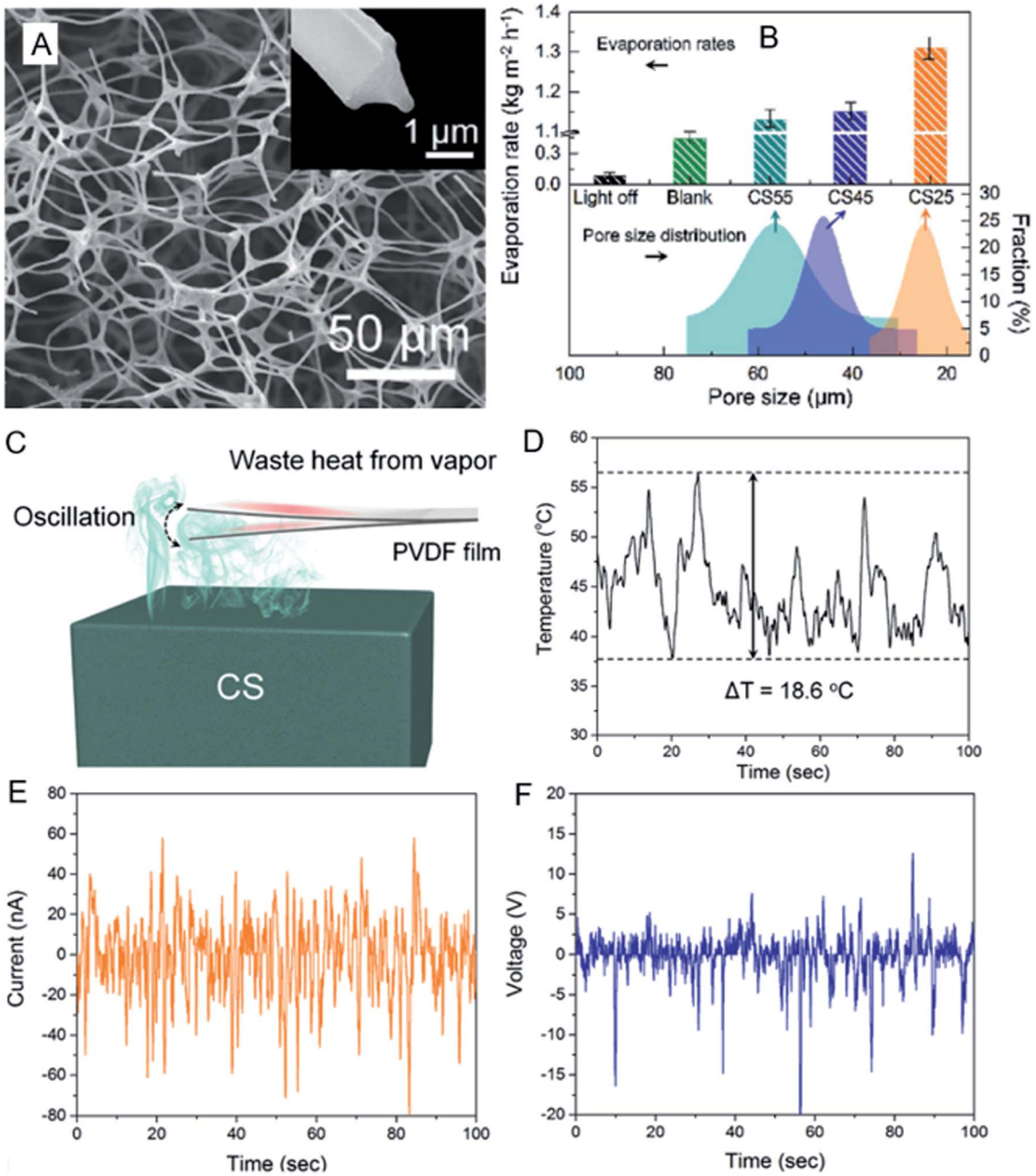

Fig. 5 (A) SEM images of carbon sponge and the high-resolution image of carbon fibrils (inset). (B) The evaporation rates and (C) the schematic of evaporation-induced potential. (D) The temperature oscillations. (E and F) Output electrical signals under solar evaporation. Reproduced with permission.[28] Copyright 2018 Wiley-VCH.

thermal energy into electricity *via* a thermoelectric device without moving parts is attractive for applications. It is conventionally believed that the use of a thermoelectric device is the most suitable method for waste heat recovery.[32,89] Recent studies demonstrate that the thermoelectric device is also attractive for converting solar energy into electricity involving high-temperature concentrating solar power[85,87,90] as well as solar evaporation at room temperature.[30,45]

Solar evaporation has been applied in wastewater treatment, desalination or distillation, solar fuel production and steam sterilization.[9,10,91] The thermoelectric module can be directly integrated with the solar absorber for harvesting thermal energy.[30,92] The module also serves as a heat insulator for improving evaporation and synchronously harvests low-grade solar heat to sustain electricity. For example, a reconfigurable solar sponge has been intentionally isolated from water by a thermoelectric module (Fig. 6a). The evaporation rates are calculated to be 1.36 and 1.20 kg m^{-2} h^{-1} (Fig. 6b), indicating the reduction of heat loss by the thermal insulation of the module. The vaporization rate decreases on decreasing the flowing water temperature, and a low temperature leads to a high thermoelectric potential of 106 mV under one-sun (Fig. 6c and d). In contrast to harvesting sensible heat, steam contains considerable latent heat of enthalpy that is normally lost to the surrounding environment. The thermoelectric module can also be used to recover steam enthalpy (Fig. 7).[45] A low-cost graphite solar absorber is used in the system (Fig. 7a and b). This absorber has broadband absorption ability (Fig. 7c) with good thermal management that leads to a high vaporization rate of 34.8 kg m^{-2} h^{-1}, corresponding to a solar-to-steam efficiency of 81.7% under 30-sun (Fig. 6e). The released heat energy is stored in a separated heat storage device above the evaporator, with temperatures of 100 °C and 25 °C at two sides (Fig. 6d). This temperature difference drives the module to generate electricity with a maximum output power of 574 mW (Fig. 6f), corresponding to a solar-to-vapor efficiency of 72.2% and power efficiency of 1.23%. The heat storage ability is the key feature of this system, which might enable electricity production at night without solar irradiation.

3.4. Thermo-electrochemical system

The thermoelectric modules are often fabricated by high-cost semiconducting materials. A thermo-electrochemical cell, also

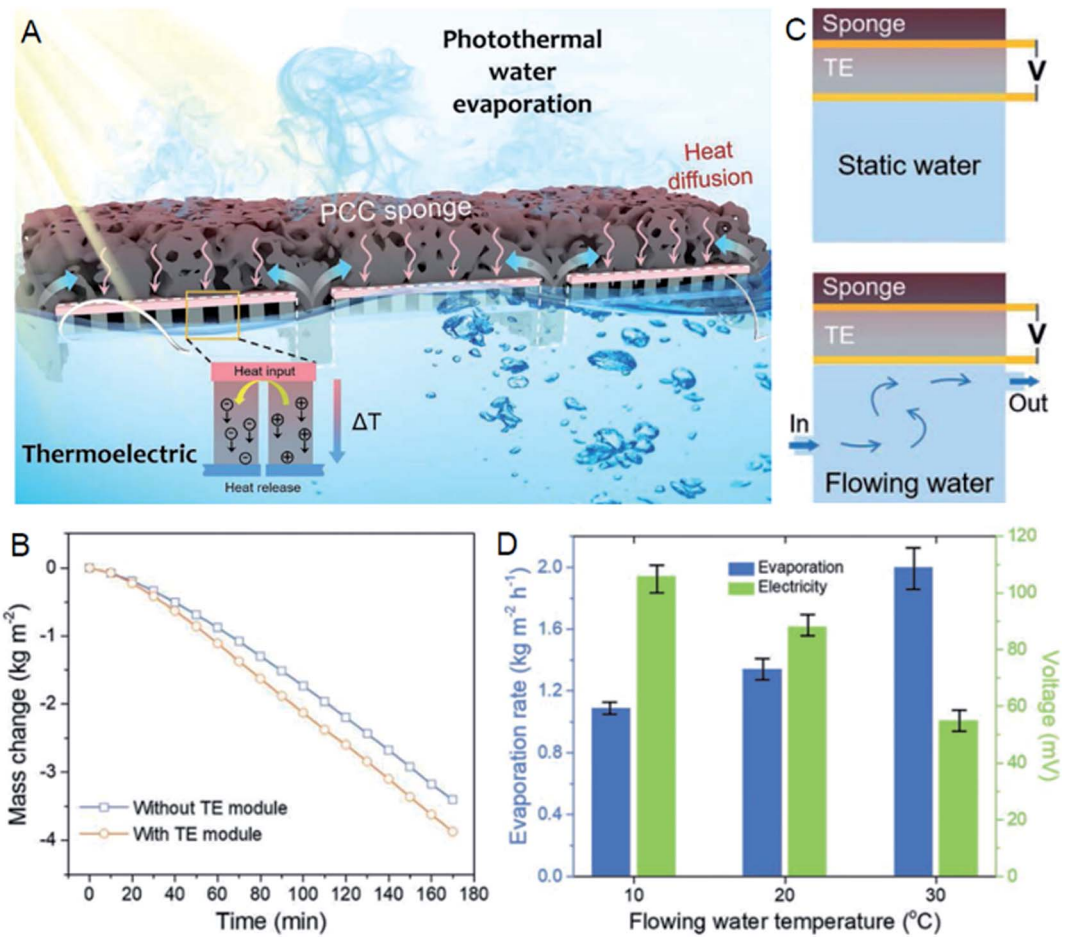

Fig. 6 (A) Solar water evaporation and thermoelectric generation. (B) The mass loss with and without the thermoelectric module. (C) Thermoelectric power generation under static and flowing water. (D) The evaporation rate and open circuit voltage of the thermoelectric module at different flowing water temperatures. Reproduced with permission.[30] Copyright 2019 Wiley-VCH.

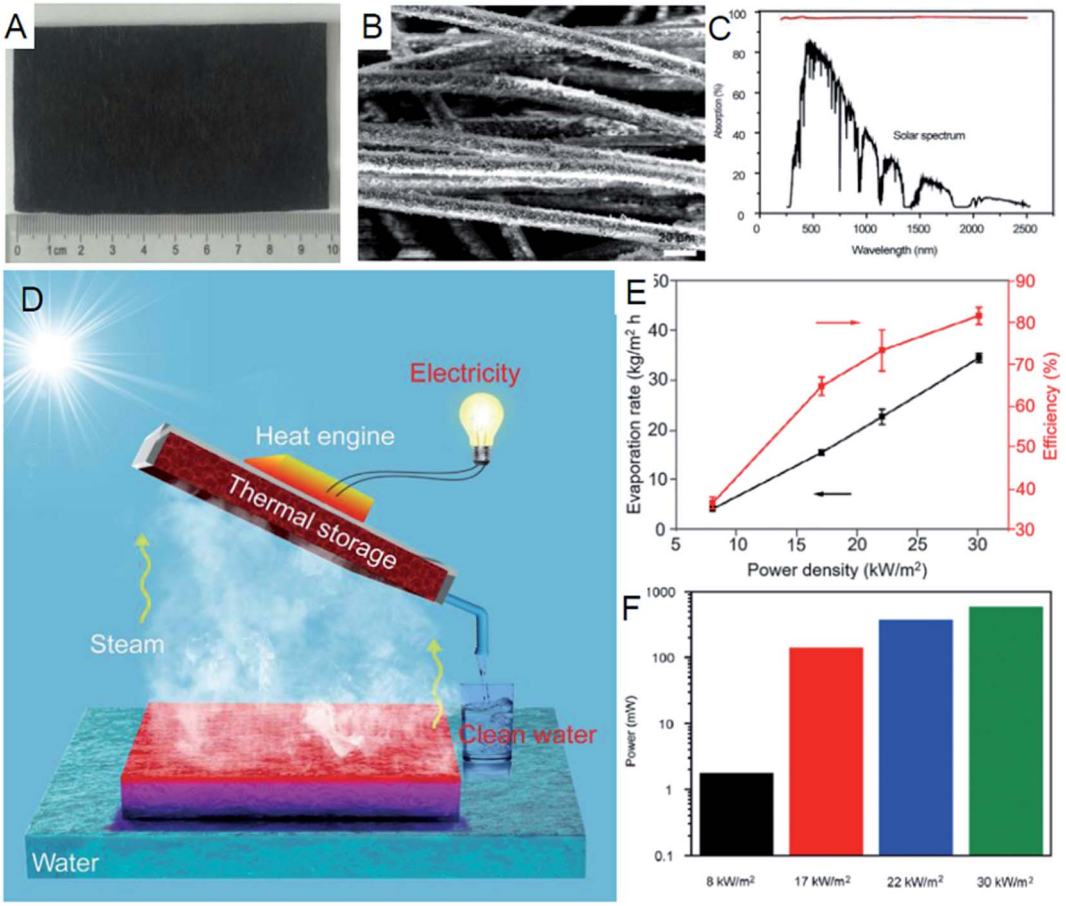

Fig. 7 (A) Optical and (B) SEM images of the light harvesting materials and (C) their solar absorption spectrum. (D) The completely thermoelectric device for both steam and power generation. (E) The vaporization rates and their corresponding solar-to-steam efficiencies. (F) Maximum power output under various light intensities. Reproduced with permission.[45] Copyright 2018 Elsevier.

known as a thermogalvanic cell, can be an alternative to the thermoelectric modules. This device requires a temperature-dependent redox couple electrolyte and electrodes to transform heat energy into electricity.[93–95] The redox reaction would occur at both the anode and the cathode, while a temperature gradient is introduced across the electrodes. The convection and migration transport of reaction species between electrodes through the electrolyte can produce a continuous current flow in the thermo-cell, building a close-cycled reaction. For a redox system $A + ne^- \leftrightarrow B$, the Seebeck coefficient can be expressed as $S = \frac{\partial V}{\partial T} = \frac{\Delta S_{B,A}}{nF}$; here, V is the electric voltage, n is the number of electrons participating in the reaction, F is the Faraday's constant, and $\Delta S_{B,A}$ denotes the reaction entropy of the electrolyte. The cell performance is determined by a new figure of merit $ZT^* = \left(\frac{z^2F^2}{R}\right)\frac{S^2 D_{lim} c}{\kappa}$; here, R is the gas constant, z is the ion charge, κ is the thermal conductivity, D_{lim} represents the diffusion coefficient and c is the electrolyte concentration.[93] Currently, two ways are used to improve power output and conversion efficiency. A large potential can be obtained by optimizing thermodynamics using electrolytes or redox couples with high Seebeck coefficients.[35,96] Current density can be amplified by the use of nanostructured electrodes as well as electrolytes with better mass transport.[94,97]

Low-cost carbon nanotube electrodes have a large surface area that is beneficial to enhance energy harvesting efficiency.[98] A graphite film has been used as both a solar absorber and a thermo-cell electrode.[29] The film is prepared from graphite fibers (Fig. 8a and b), and the fibers exhibit hydrophilic properties with a contact angle approaching to zero. The film has a broadband solar absorption from 250 to 2500 nm, as shown in Fig. 8c. Fig. 8d shows the thermo-electrochemical system enabled by interfacial solar evaporation. The redox couple of the system is the I^{3-}/I^- ion pair that has distinct temperature-dependent redox potentials. When exposed to solar irradiation, a temperature gradient across the electrodes would create a redox potential difference in the electrolyte to produce electricity. Both DI water and seawater electrolytes were employed in the system. It was found that the vaporization rate was greatly improved as compared to that for the system without the absorber (Fig. 8e). The evaporation rate with the seawater electrolyte reached 1.1 kg m^{-2} h^{-1}, corresponding to a solar-to-steam efficiency of ~60%. The output power was about 0.5 mW m^{-2}, and it still retained about ~0.023 mW m^{-2} even at night without light illumination. This opens a new avenue for power

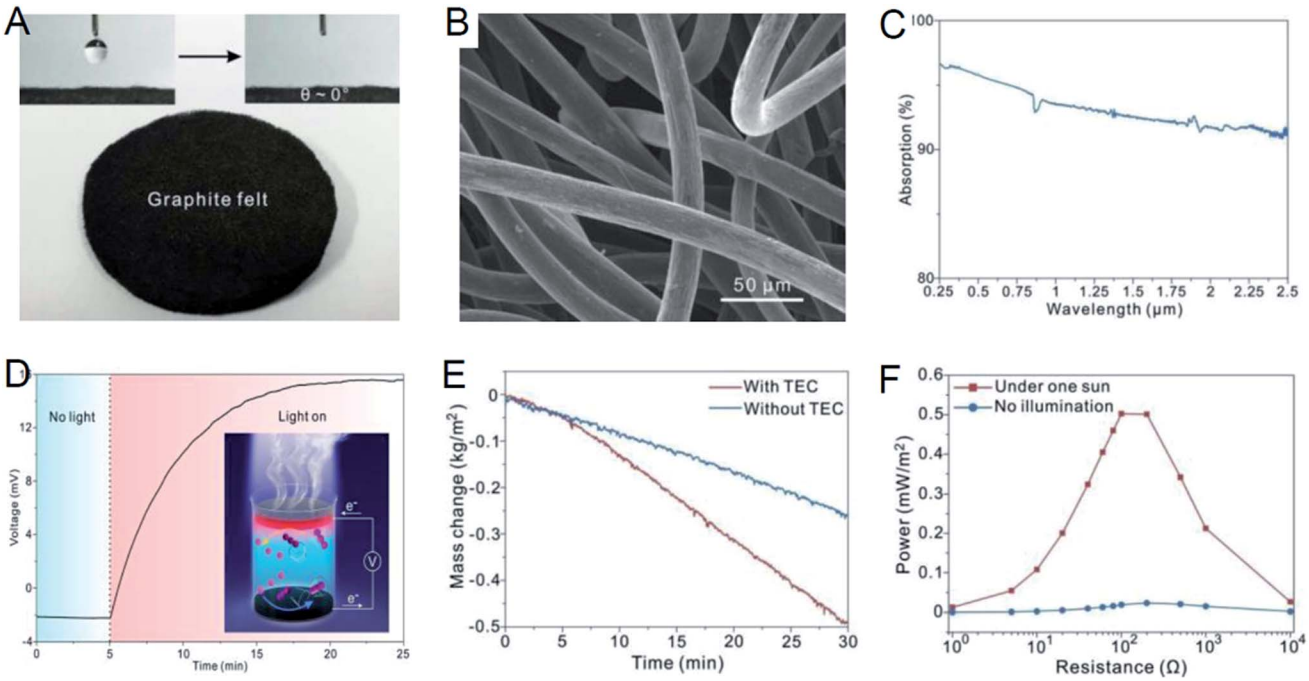

Fig. 8 Graphite film parallel functions as the solar absorber and the thermo-cell electrode. (A) Optical and (B) SEM images of the film. (C) The absorption spectrum. (D) The thermo-electrochemical cell for clean water and electricity generation. (E) Mass loss curves *versus* time. (F) Output power with and without solar illumination. Reproduced with permission.[29] Copyright 2019 Royal Society of Chemistry.

generation driven by a temperature difference from natural evaporation.

3.5. Salinity power system

The salinity difference between seawater and fresh water stores a great amount of renewable energy.[18,99] The so-called "blue energy" can be extracted in the mixing process of seawater and fresh water. In theory, maximum work released from mixing can be evaluated by the Gibbs free energy ΔG_{mix}. The Gibbs free energy difference per unit volume *via* mixing is calculated as $\Delta G_{mix} = RT[c_m \ln(c_m) - \chi c_s \ln(c_s) - (1-\chi)c_r \ln(c_r)]$, where χ is the volumetric fraction of seawater, c_m denotes the concentration of mixed solution, c_s is the concentration of seawater, and c_r is the concentration of river water.[37,100] The useful work produced by the unit in practical applications is always less than the Gibbs free energy due to the inevitably produced entropy.[37,101] The prevalent technologies to harvest salinity energy are reverse electrodialysis,[36,102] pressure retarded osmosis[103] and electric double-layer capacitors.[100,104] In reverse electrodialysis, the chemical potential gradient drives a directional transport of charges across ion-exchange membranes to produce electricity. Salt-rejecting membranes are used in pressure retarded osmosis to create an osmotic pressure difference between the two solutions to drive power generation. In capacitive energy harvesting, the cycling-varied potential is a result of alternating a porous electrode pair in electrolytes at different concentrations to convert salinity energy into useful work.

Solar evaporation brings new chances to deal with the water-energy crisis.[20,105,106] To concurrently harvest solar and salinity energies, Zhou *et al.* developed a hybrid system for demonstrating solar evaporation and salinity power (Fig. 9a and b).[27] Under illumination, the carbon-based absorber converted solar energy to heat, leading to a localized high temperature and thus, vapor was easily released *via* evaporation. Seawater is continuously transported to the evaporative surface by the capillary force of the paper. This rapid evaporation inevitably poses a salinity difference across the membrane, which thus promotes a directional charge transport to produce electricity. Fig. 9c illustrates the energy flux of evaporation. The final device generates an electrical power of 1 W m^{-2}, with a solar-to-vapor efficiency of 75% under one sun. Theoretically, the power generation from this method can approach 12.5 W m^{-2}, while the actual electric power is less than 10% because ions do not pass through the membrane. A scalable device was also developed to further verify the design (Fig. 9d and e). Owing to a natural convection environment, the vaporization rate can reach 1.1 kg m^{-2} h^{-1}. The open-circuit potential is ~66 mV and an optimized power of 3 mW can be obtained under a steady-state operation (Fig. 9f). Moreover, they also reported water evaporation-induced electricity in porous carbon films.[22,107,108] The conceptual device consists of a carbon black film and two carbon nanotube electrodes, which can produce a sustained potential of ~1.0 V under natural evaporation.[22] The evaporation-driven water flow contributes to the strong interaction of water molecules with carbon materials that is responsible for power generation.[26,109] However, this system is unable to collect condensed water and harvest steam thermal energy. Nevertheless, the works offer novel insights for blue energy harvesting, demonstrating the potential for wide applications of the technology.

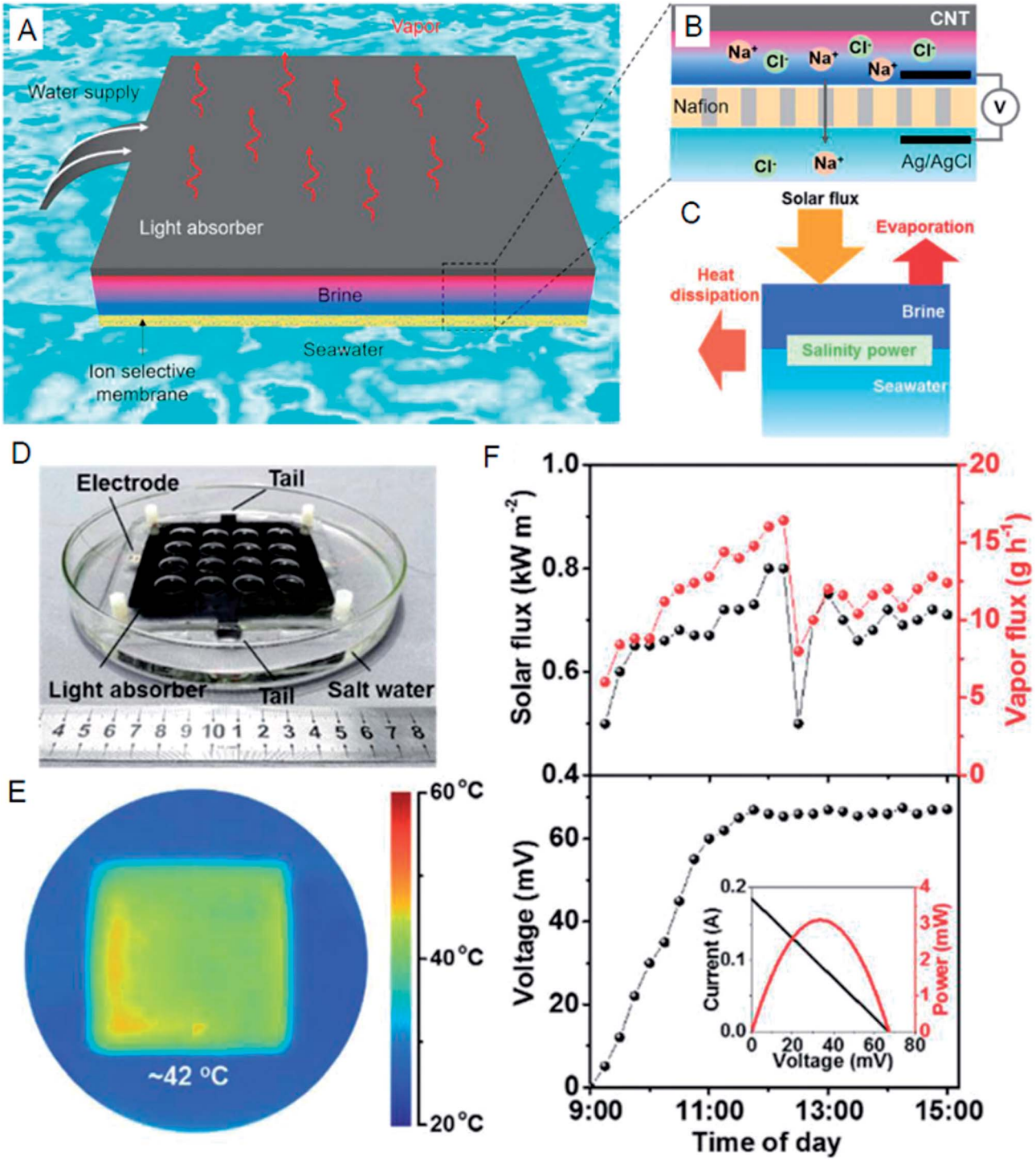

Fig. 9 (A) Steam and power generation from salinity. (B) Mechanism and (C) energy flux of the solar hybrid system. (D) A photograph of the scalable device. (E) The IR image of surface under natural irradiation. (F) The solar and vapor flux (upper panel) as well as the electrical output (lower panel). Reproduced with permission.[27] Copyright 2019 Royal Society of Chemistry.

4. Summary and prospects

This work summarizes the progress on interfacial solar evaporation for fresh water production simultaneously towards waste energy harvesting through triboelectric, pyroelectric, piezoelectric, thermoelectric, thermal-electrochemical and salinity effects. The photothermal physics and engineering strategies of solar materials were briefly described for advanced solar energy harvesting. The interaction of photothermal materials and steam devices with electricity producing systems was then addressed. Table 1 shows a summary of the energy harvesting mechanisms, absorber materials, photothermal physics,

evaporation and electricity generation performances, and their potential applications in a wide range of water–energy nexus, *e.g.*, water desalination, thermal energy storage, waste material utilization, electricity generation, *etc.* The input energy sources are various and can be mechanical, thermal, or chemical energy or their hybrid scheme from time to time. Some developed systems have shown the capability to overcome the intermittent nature of solar evaporation.[22,29,45] The typical evaporation rates and solar-to-steam efficiencies were extracted from selected articles and are shown in Fig. 10a. Power density and output potential are key parameters to define the total energy and threshold voltage of a device; they are highlighted in Fig. 10b. This can hopefully provide a global insight on the pros and cons of energy harvesting mechanisms as well as the solar hybrid technologies they potentially would enable. It was concluded that the high vaporization rate above 1.1 kg m^{-2} h^{-1} could be easily achieved through the rational scrutinization of photothermal materials and careful engineering of solar absorbers and evaporators. Solar-to-steam efficiency approaching 90% can also be expected in the hybrid system with extra power generated simultaneously. A high voltage can result from the triboelectric and piezoelectric effects, while a high current can often be produced by the thermoelectric or salinity effect. Although there is growing interest in the potential for scale-up applications, the voltages are high (low) and the currents are normally low (high), which limit the power output. Overall, the progress of coupling interfacial solar evaporation with power generation shows great prospects in addressing water-energy challenges.[110] We believe that this solar hybrid technology would attract more attention in the near future.

The remaining challenges in the fields include mechanistic elucidation, material manipulation, device structure optimization and integration, and improvement in the steam energy level and power density for practical operations. To expand opportunities in this interdisciplinary field, there is a need for the mechanistic understanding of how localized heating and water and vapor flow affect the steam and power generation performance. Highly efficient photothermal materials and floating insulation materials that are commercially available should be scrutinized and produced at a low cost. The influence of the micro/nanostructure design and surface chemistry of a solar absorber, evaporation structure and thermal insulator on both performances needs to be further explored systematically. To enhance the clean water flux and power density of the system, scaling up the evaporator/generator device either in dimensions or in quantity can be beneficial. A solar evaporator/generator network represents a feasible strategy.[111] The connection of units in series would increase the open-circuit voltage, and parallel connection would increase the short-circuit current.[22,112] Networks linking large numbers of units *via* cables can be floated on an ocean surface for both seawater desalination and blue energy harvesting. This scheme can in principle be implemented at a scale comparable to that of photovoltaics for solar energy harvesting. Another potential strategy is to use the PV technology or concentrated sunlight to enhance the evaporation and power density at the same time.[76,78,113] This reflects that the techniques used in other solar energy fields can be introduced to the solar hybrid systems.[3,87,114] Moreover, integrating solar thermal energy storage technologies into the systems can help address the solar intermittency issue.[45,115]

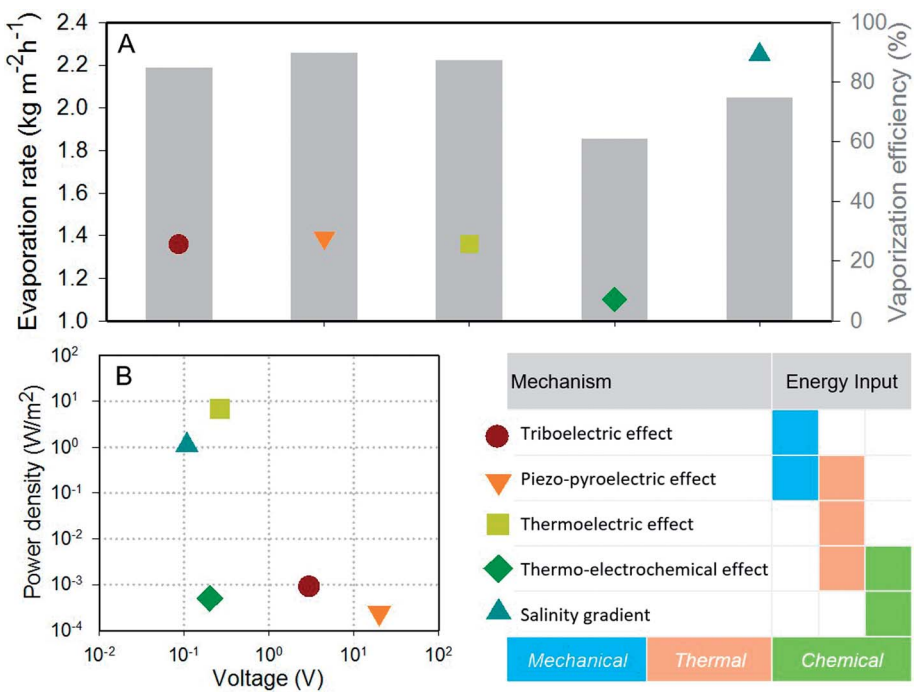

Fig. 10 (A) The reported vaporization rates and solar-to-steam efficiencies of solar hybrid systems. (B) A global plot to highlight the power density and open-circuit voltage according to the energy harvesting mechanism.

Inspired by the reported systems, we propose two new concepts of a device here for further development. The first prototype consists of three essential components: a photothermal sponge, a Joule heating film and a thermoelectric module. As shown in Fig. 11, the thermoelectric module and heating film are integrated on the supporting sponge to make the device float on the seawater surface. The solar sponge has high optical absorption and favorable inbuilt micro/nanostructures, which are desirable for photothermal conversion, efficient fluid transport and heat management. The top side of the thermoelectric device is carpeted by the heating film and the solar sponge to create the hot side by localizing solar heating as well as Joule heating. The temperature difference between the sponge and the water present underneath drives the thermoelectric module to harvest low-grade heat for waste heat-to-electricity conversion. The produced electricity is *in situ* used to heat the Joule film, which further improves the temperature of the sponge.[116,117] Meanwhile, the thermoelectric module also functions as a thermal insulator under the sponge to enhance solar evaporation. As a result, solar energy can be more efficiently transformed into heat energy for water evaporation by the synergistic coupling of the photothermal effect with the thermoelectric technology. Another potential device is composed of a thermo-electrochemical cell embedded in a bubble-column evaporator that is linked with a condenser for concurrent water production and heat recovery (Fig. 12).[118] The meshed black material acts as both the solar absorber and the thermo-cell electrode. The generated electricity can be *in situ* used to drive the pump for air bubbling to enhance the mass transfer of humidification or to satisfy other power supplies in off-grid areas. Such desalination and electricity technologies not only overcome the fouling issues that can hinder device operation, but also fully utilize the waste heat from both water and vapor, which would be significant for more energy saving and large-scale applications.

Due to the abundance of solar energy and widely distributed water resources, solar evaporation can also be a promising technology toward resource production.[119,120] The combination

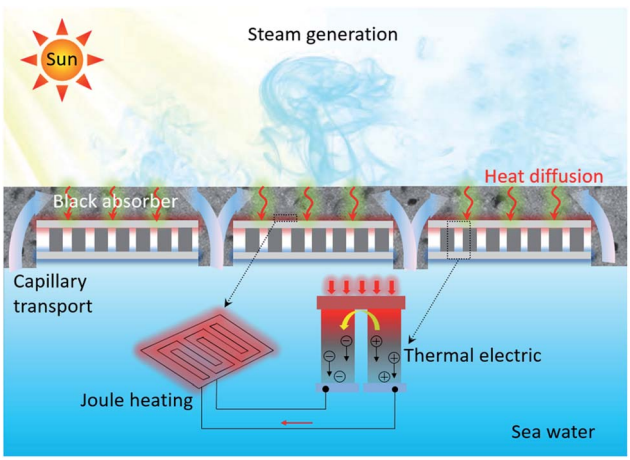

Fig. 11 A solar steam device towards enhanced evaporation *via* direct photothermal-thermoelectric coupling.

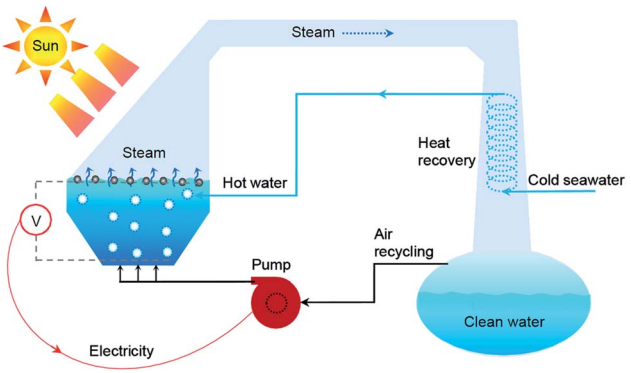

Fig. 12 A new concept of solar evaporation for clean water and renewable energy.

of new functions into the existing energy frameworks for further grid-scale applications will be the next research focus, *e.g.*, the interdisciplinary coupling of refuse burning, geothermal heat and photovoltaics at a large-scale is valuable to build a Synergy City (Fig. 13).[113,121] A variety of heat sources can be used to produce steam for the generator. This requires multiple generators that can be run in series or parallel, *e.g.*, solar energy is not available at night and hereby, refuse burning, geothermal heat and possibly other sources would pick up the load. The thermal cycle requires a heat sink to discharge the rejected heat and such sinks can be rivers, lakes, cooling towers or even a large man-made lake, in which freshwater flows in from the desalination plants processing sea water. Such plants can be located at the sources using power produced locally or from a Synergy City. This kind of city can be a man-made oasis, which is presently uninhabitable, enhancing the environment and offering employment opportunities. More importantly, the Synergy City has a potential to solve the major issues confronting our society: (i) the need for freshwater in arid regions; (ii) the need for power production from environmentally safe sources; and (iii) the need to safely dispose of trash from communities. With this vision and dream, the intrinsic advantages of interfacial solar evaporation would not only accelerate the harvesting and utilization of solar energy, but

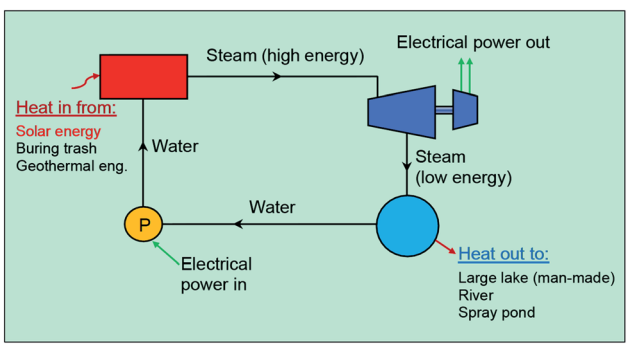

Fig. 13 Vision of solar evaporation in the development of a Synergy City. Reproduced with permission.[121] Copyright 2011 United States Patent Office.

also inspire new translation of the technology into other energy frameworks towards a better future.

Conflicts of interest

The authors declare no competing financial interests.

Acknowledgements

The research was supported by grants from the Natural Science Foundation of China (51576002 and 51436004).

References

1 J. B. K. a. S. C. Stultz, *Steam Its Generation and use, Edition 41*, Copyright© by The Babcock & Wilcox Company a McDermott company, 2005.
2 M. I. Hoffert, K. Caldeira, G. Benford, D. R. Criswell, C. Green, H. Herzog, A. K. Jain, H. S. Kheshgi, K. S. Lackner, J. S. Lewis, H. D. Lightfoot, W. Manheimer, J. C. Mankins, M. E. Mauel, L. J. Perkins, M. E. Schlesinger, T. Volk and T. M. Wigley, Advanced technology paths to global climate stability: energy for a greenhouse planet, *Science*, 2002, **298**, 981–987.
3 L. A. Weinstein, J. Loomis, B. Bhatia, D. M. Bierman, E. N. Wang and G. Chen, Concentrating Solar Power, *Chem. Rev.*, 2015, **115**, 12797–12838.
4 N. S. Lewis, Research opportunities to advance solar energy utilization, *Science*, 2016, **351**, aad1920.
5 P. Tao, G. Ni, C. Song, W. Shang, J. Wu, J. Zhu, G. Chen and T. Deng, Solar-driven interfacial evaporation, *Nat. Energy*, 2018, **3**, 1031–1041.
6 W. Shang and T. Deng, Solar steam generation: Steam by thermal concentration, *Nat. Energy*, 2016, **1**, 16133.
7 H. Liu, Z. Huang, K. Liu, X. Hu and J. Zhou, Interfacial Solar-to-Heat Conversion for Desalination, *Adv. Energy Mater.*, 2019, **9**, 1900310.
8 G. Liu, J. Xu and K. Wang, Solar water evaporation by black photothermal sheets, *Nano Energy*, 2017, **41**, 269–284.
9 M. Gao, L. Zhu, C. K. Peh and G. W. Ho, Solar absorber material and system designs for photothermal water vaporization towards clean water and energy production, *Energy Environ. Sci.*, 2019, **12**, 841–864.
10 C. Chen, Y. Kuang and L. Hu, Challenges and Opportunities for Solar Evaporation, *Joule*, 2019, **3**, 683–718.
11 P. Zhang, Q. Liao, H. Yao, Y. Huang, H. Cheng and L. Qu, Direct solar steam generation system for clean water production, *Energy Storage Materials*, 2019, **18**, 429–446.
12 X. Wang, Q. Liu, S. Wu, B. Xu and H. Xu, Multilayer Polypyrrole Nanosheets with Self-Organized Surface Structures for Flexible and Efficient Solar-Thermal Energy Conversion, *Adv. Mater.*, 2019, **31**, e1807716.
13 J. Chen, J. Feng, Z. Li, P. Xu, X. Wang, W. Yin, M. Wang, X. Ge and Y. Yin, Space-Confined Seeded Growth of Black Silver Nanostructures for Solar Steam Generation, *Nano Lett.*, 2019, **19**, 400–407.
14 F. Zhao, X. Zhou, Y. Shi, X. Qian, M. Alexander, X. Zhao, S. Mendez, R. Yang, L. Qu and G. Yu, Highly efficient solar vapour generation via hierarchically nanostructured gels, *Nat. Nanotechnol.*, 2018, **13**, 489–495.
15 A. H. Cavusoglu, X. Chen, P. Gentine and O. Sahin, Potential for natural evaporation as a reliable renewable energy resource, *Nat. Commun.*, 2017, **8**, 617.
16 Z. Zhang, X. Li, J. Yin, Y. Xu, W. Fei, M. Xue, Q. Wang, J. Zhou and W. Guo, Emerging hydrovoltaic technology, *Nat. Nanotechnol.*, 2018, **13**, 1109–1119.
17 G. Liu, T. Chen, J. Xu and K. Wang, Blue energy harvesting on nanostructured carbon materials, *J. Mater. Chem. A*, 2018, **6**, 18357–18377.
18 B. E. Logan and M. Elimelech, Membrane-based processes for sustainable power generation using water, *Nature*, 2012, **488**, 313–319.
19 X. Chen, D. Goodnight, Z. Gao, A. H. Cavusoglu, N. Sabharwal, M. DeLay, A. Driks and O. Sahin, Scaling up nanoscale water-driven energy conversion into evaporation-driven engines and generators, *Nat. Commun.*, 2015, **6**, 7346.
20 A. P. Straub, N. Y. Yip, S. Lin, J. Lee and M. Elimelech, Harvesting low-grade heat energy using thermo-osmotic vapour transport through nanoporous membranes, *Nat. Energy*, 2016, **1**, 16090.
21 Z. Wang, T. Horseman, A. P. Straub, N. Y. Yip, D. Li, M. Elimelech and S. Lin, Pathways and challenges for efficient solar-thermal desalination, *Science advances*, 2019, **5**, eaax0763.
22 G. Xue, Y. Xu, T. Ding, J. Li, J. Yin, W. Fei, Y. Cao, J. Yu, L. Yuan, L. Gong, J. Chen, S. Deng, J. Zhou and W. Guo, Water-evaporation-induced electricity with nanostructured carbon materials, *Nat. Nanotechnol.*, 2017, **12**, 317–321.
23 C. Li, K. Liu, H. Liu, B. Yang and X. Hu, Capillary driven electrokinetic generator for environmental energy harvesting, *Mater. Res. Bull.*, 2017, **90**, 81–86.
24 B. Hou, D. Kong, J. Qian, Y. Yu, Z. Cui, X. Liu, J. Wang, T. Mei, J. Li and X. Wang, Flexible and portable graphene on carbon cloth as a power generator for electricity generation, *Carbon*, 2018, **140**, 488–493.
25 G. Zhang, Z. Duan, X. Qi, Y. Xu, L. Li, W. Ma, H. Zhang, C. Liu and W. Yao, Harvesting environment energy from water-evaporation over free-standing graphene oxide sponges, *Carbon*, 2019, **148**, 1–8.
26 T. Mouterde, A. Keerthi, A. R. Poggioli, S. A. Dar, A. Siria, A. K. Geim, L. Bocquet and B. Radha, Molecular streaming and its voltage control in angstrom-scale channels, *Nature*, 2019, **567**, 87–90.
27 P. Yang, K. Liu, Q. Chen, J. Li, J. Duan, G. Xue, Z. Xu, W. Xie and J. Zhou, Solar-driven simultaneous steam production and electricity generation from salinity, *Energy Environ. Sci.*, 2017, **10**, 1923–1927.
28 L. Zhu, M. Gao, C. K. N. Peh, X. Wang and G. W. Ho, Self-Contained Monolithic Carbon Sponges for Solar-Driven Interfacial Water Evaporation Distillation and Electricity Generation, *Adv. Energy Mater.*, 2018, **8**, 1702149.

29 Q. C. Shen, Z. Y. Ning, B. W. Fu, S. Ma, Z. Y. Wang, L. Shu, L. F. Zhang, X. Y. Wang, J. L. Xu, P. Tao, C. Y. Song, J. B. Wu, T. Deng and W. Shang, An open thermo-electrochemical cell enabled by interfacial evaporation, *J. Mater. Chem. A*, 2019, **7**, 6514–6521.

30 L. Zhu, T. Ding, M. Gao, C. K. N. Peh and G. W. Ho, Shape Conformal and Thermal Insulative Organic Solar Absorber Sponge for Photothermal Water Evaporation and Thermoelectric Power Generation, *Adv. Energy Mater.*, 2019, 1900250.

31 Z. L. Wang, J. Chen and L. Lin, Progress in triboelectric nanogenerators as a new energy technology and self-powered sensors, *Energy Environ. Sci.*, 2015, **8**, 2250–2282.

32 L. E. Bell, Cooling, heating, generating power, and recovering waste heat with thermoelectric systems, *Science*, 2008, **321**, 1457–1461.

33 S. Pandya, J. Wilbur, J. Kim, R. Gao, A. Dasgupta, C. Dames and L. W. Martin, Pyroelectric energy conversion with large energy and power density in relaxor ferroelectric thin films, *Nature materials*, 2018, **17**, 432–438.

34 Z. L. Wang and J. Song, Piezoelectric nanogenerators based on zinc oxide nanowire arrays, *Science*, 2006, **312**, 242–246.

35 J. Duan, G. Feng, B. Yu, J. Li, M. Chen, P. Yang, J. Feng, K. Liu and J. Zhou, Aqueous thermogalvanic cells with a high Seebeck coefficient for low-grade heat harvest, *Nat. Commun.*, 2018, **9**, 5146.

36 J. Gao, W. Guo, D. Feng, H. Wang, D. Zhao and L. Jiang, High-performance ionic diode membrane for salinity gradient power generation, *J. Am. Chem. Soc.*, 2014, **136**, 12265–12272.

37 N. Y. Yip, D. Brogioli, H. V. Hamelers and K. Nijmeijer, Salinity Gradients for Sustainable Energy: Primer, Progress, and Prospects, *Environ. Sci. Technol.*, 2016, **50**, 12072–12094.

38 M. L. Brongersma, N. J. Halas and P. Nordlander, Plasmon-induced hot carrier science and technology, *Nat. Nanotechnol.*, 2015, **10**, 25–34.

39 Y. Yang, X. Yang, L. Fu, M. Zou, A. Cao, Y. Du, Q. Yuan and C.-H. Yan, Two-Dimensional Flexible Bilayer Janus Membrane for Advanced Photothermal Water Desalination, *ACS Energy Lett.*, 2018, **3**, 1165–1171.

40 J. R. Vélez-Cordero and J. Hernández-Cordero, Heat generation and conduction in PDMS-carbon nanoparticle membranes irradiated with optical fibers, *Int. J. Therm. Sci.*, 2015, **96**, 12–22.

41 C. M. Hessel, V. P. Pattani, M. Rasch, M. G. Panthani, B. Koo, J. W. Tunnell and B. A. Korgel, Copper selenide nanocrystals for photothermal therapy, *Nano Lett.*, 2011, **11**, 2560–2566.

42 J. Wang, Y. Li, L. Deng, N. Wei, Y. Weng, S. Dong, D. Qi, J. Qiu, X. Chen and T. Wu, High-Performance Photothermal Conversion of Narrow-Bandgap Ti_2O_3 Nanoparticles, *Adv. Mater.*, 2017, **29**, 1603730.

43 Y. Kuang, C. Chen, S. He, E. M. Hitz, Y. Wang, W. Gan, R. Mi and L. Hu, A High-Performance Self-Regenerating Solar Evaporator for Continuous Water Desalination, *Adv. Mater.*, 2019, **31**, e1900498.

44 Q. Jiang and S. Singamaneni, Water from Wood: Pouring through Pores, *Joule*, 2017, **1**, 429–430.

45 X. Li, X. Min, J. Li, N. Xu, P. Zhu, B. Zhu, S. Zhu and J. Zhu, Storage and Recycling of Interfacial Solar Steam Enthalpy, *Joule*, 2018, **2**, 2477–2484.

46 K. Mizuno, J. Ishii, H. Kishida, Y. Hayamizu, S. Yasuda, D. N. Futaba, M. Yumura and K. Hata, A black body absorber from vertically aligned single-walled carbon nanotubes, *Proc. Natl. Acad. Sci. U. S. A.*, 2009, **106**, 6044–6047.

47 S. Thongrattanasiri, F. H. Koppens and F. J. Garcia de Abajo, Complete optical absorption in periodically patterned graphene, *Phys. Rev. Lett.*, 2012, **108**, 047401.

48 H. Ren, M. Tang, B. Guan, K. Wang, J. Yang, F. Wang, M. Wang, J. Shan, Z. Chen, D. Wei, H. Peng and Z. Liu, Hierarchical Graphene Foam for Efficient Omnidirectional Solar-Thermal Energy Conversion, *Adv. Mater.*, 2017, **29**, 1702590.

49 H. K. Raut, V. A. Ganesh, A. S. Nair and S. Ramakrishna, Anti-reflective coatings: A critical, in-depth review, *Energy Environ. Sci.*, 2011, **4**, 3779.

50 X. Zheng and L. Zhang, Photonic nanostructures for solar energy conversion, *Energy Environ. Sci.*, 2016, **9**, 2511–2532.

51 A. O. Govorov and H. H. Richardson, Generating heat with metal nanoparticles, *Nano Today*, 2007, **2**, 30–38.

52 H. H. Richardson, M. T. Carlson, P. J. Tandler, P. Hernandez and A. O. Govorov, Experimental and theoretical studies of light-to-heat conversion and collective heating effects in metal nanoparticle solutions, *Nano Lett.*, 2009, **9**, 1139–1146.

53 N. Jiang, X. Zhuo and J. Wang, Active Plasmonics: Principles, Structures, and Applications, *Chem. Rev.*, 2018, **118**, 3054–3099.

54 N. Zhang, C. Han, X. Fu and Y.-J. Xu, Function-Oriented Engineering of Metal-Based Nanohybrids for Photoredox Catalysis: Exerting Plasmonic Effect and Beyond, *Chem*, 2018, **4**, 1832–1861.

55 G. Liu, K. Du, J. Xu, G. Chen, M. Gu, C. Yang, K. Wang and H. Jakobsen, Plasmon-dominated photoelectrodes for solar water splitting, *J. Mater. Chem. A*, 2017, **5**, 4233–4253.

56 M. B. Ross, M. G. Blaber and G. C. Schatz, Using nanoscale and mesoscale anisotropy to engineer the optical response of three-dimensional plasmonic metamaterials, *Nat. Commun.*, 2014, **5**, 4090.

57 M. S. Zielinski, J. W. Choi, T. La Grange, M. Modestino, S. M. Hashemi, Y. Pu, S. Birkhold, J. A. Hubbell and D. Psaltis, Hollow Mesoporous Plasmonic Nanoshells for Enhanced Solar Vapor Generation, *Nano Lett.*, 2016, **16**, 2159–2167.

58 Y. Wang, D. Wan, S. Xie, X. Xia, C. Z. Huang and Y. Xia, Synthesis of silver octahedra with controlled sizes and optical properties via seed-mediated growth, *ACS Nano*, 2013, **7**, 4586–4594.

59 L. Zhang, H. Jing, G. Boisvert, J. Z. He and H. Wang, Geometry control and optical tunability of metal-cuprous oxide core-shell nanoparticles, *ACS Nano*, 2012, **6**, 3514–3527.

60 K. Bae, G. Kang, S. K. Cho, W. Park, K. Kim and W. J. Padilla, Flexible thin-film black gold membranes with ultrabroadband plasmonic nanofocusing for efficient solar vapour generation, *Nat. Commun.*, 2015, **6**, 10103.

61 L. Zhou, Y. Tan, D. Ji, B. Zhu, P. Zhang, J. Xu, Q. Gan, Z. Yu and J. Zhu, Self-assembly of highly efficient, broadband plasmonic absorbers for solar steam generation, *Science advances*, 2016, **2**, e1501227.

62 L. Zhou, Y. Tan, J. Wang, W. Xu, Y. Yuan, W. Cai, S. Zhu and J. Zhu, 3D self-assembly of aluminium nanoparticles for plasmon-enhanced solar desalination, *Nat. Photonics*, 2016, **10**, 393–398.

63 M. Ye, J. Jia, Z. Wu, C. Qian, R. Chen, P. G. O'Brien, W. Sun, Y. Dong and G. A. Ozin, Synthesis of Black TiO_x Nanoparticles by Mg Reduction of TiO_2 Nanocrystals and their Application for Solar Water Evaporation, *Adv. Energy Mater.*, 2017, **7**, 1601811.

64 C. Zhang, C. Yan, Z. Xue, W. Yu, Y. Xie and T. Wang, Shape-Controlled Synthesis of High-Quality Cu_7S_4 Nanocrystals for Efficient Light-Induced Water Evaporation, *Small*, 2016, **12**, 5320–5328.

65 J. Li and N. Wu, Semiconductor-based photocatalysts and photoelectrochemical cells for solar fuel generation: a review, *Catal. Sci. Technol.*, 2015, **5**, 1360–1384.

66 Z. Zhang, Y. Wang, P. A. Stensby Hansen, K. Du, K. R. Gustavsen, G. Liu, F. Karlsen, O. Nilsen, C. Xue and K. Wang, Black silicon with order-disordered structures for enhanced light trapping and photothermic conversion, *Nano Energy*, 2019, **65**, 103992.

67 Y. Zeng, J. Yao, B. A. Horri, K. Wang, Y. Wu, D. Li and H. Wang, Solar evaporation enhancement using floating light-absorbing magnetic particles, *Energy Environ. Sci.*, 2011, **4**, 4074.

68 R. Chen, Z. Wu, T. Zhang, T. Yu and M. Ye, Magnetically recyclable self-assembled thin films for highly efficient water evaporation by interfacial solar heating, *RSC Adv.*, 2017, **7**, 19849–19855.

69 P. Wang, Emerging investigator series: the rise of nano-enabled photothermal materials for water evaporation and clean water production by sunlight, *Environ. Sci.: Nano*, 2018, **5**, 1078–1089.

70 R. Bleischwitz, C. Spataru, S. D. VanDeveer, M. Obersteiner, E. van der Voet, C. Johnson, P. Andrews-Speed, T. Boersma, H. Hoff and D. P. van Vuuren, Resource nexus perspectives towards the United Nations Sustainable Development Goals, *Nature Sustainability*, 2018, **1**, 737–743.

71 M. Gao, C. K. Peh, H. T. Phan, L. Zhu and G. W. Ho, Solar Absorber Gel: Localized Macro-Nano Heat Channeling for Efficient Plasmonic Au Nanoflowers Photothermic Vaporization and Triboelectric Generation, *Adv. Energy Mater.*, 2018, **8**, 1800711.

72 F.-R. Fan, Z.-Q. Tian and Z. Lin Wang, Flexible triboelectric generator, *Nano Energy*, 2012, **1**, 328–334.

73 S. Niu and Z. L. Wang, Theoretical systems of triboelectric nanogenerators, *Nano Energy*, 2015, **14**, 161–192.

74 Z. L. Wang, On Maxwell's displacement current for energy and sensors: the origin of nanogenerators, *Mater. Today*, 2017, **20**, 74–82.

75 J.-H. Lee, J. Kim, T. Y. Kim, M. S. Al Hossain, S.-W. Kim and J. H. Kim, All-in-one energy harvesting and storage devices, *J. Mater. Chem. A*, 2016, **4**, 7983–7999.

76 S.-B. Jeon, D. Kim, G.-W. Yoon, J.-B. Yoon and Y.-K. Choi, Self-cleaning hybrid energy harvester to generate power from raindrop and sunlight, *Nano Energy*, 2015, **12**, 636–645.

77 L. Zheng, Z.-H. Lin, G. Cheng, W. Wu, X. Wen, S. Lee and Z. L. Wang, Silicon-based hybrid cell for harvesting solar energy and raindrop electrostatic energy, *Nano Energy*, 2014, **9**, 291–300.

78 J. Duan, T. Hu, Y. Zhao, B. He and Q. Tang, Carbon-Electrode-Tailored All-Inorganic Perovskite Solar Cells To Harvest Solar and Water-Vapor Energy, *Angew. Chem.*, 2018, **57**, 5746–5749.

79 L. Xu, T. Jiang, P. Lin, J. J. Shao, C. He, W. Zhong, X. Y. Chen and Z. L. Wang, Coupled Triboelectric Nanogenerator Networks for Efficient Water Wave Energy Harvesting, *ACS Nano*, 2018, **12**, 1849–1858.

80 J. Briscoe and S. Dunn, Piezoelectric nanogenerators - a review of nanostructured piezoelectric energy harvesters, *Nano Energy*, 2015, **14**, 15–29.

81 S. R. Hunter, N. V. Lavrik, S. Mostafa, S. Rajic and P. G. Datskos, Review of pyroelectric thermal energy harvesting and new MEMs-based resonant energy conversion techniques, Energy Harvesting and Storage: Materials, Devices, and Applications III, *Proc. SPIE*, 2012, **8377**, 83770D–83771D.

82 Y. Zhang, M. Xie, V. Adamaki, H. Khanbareh and C. R. Bowen, Control of electro-chemical processes using energy harvesting materials and devices, *Chem. Soc. Rev.*, 2017, **46**, 7757–7786.

83 P. Talemi, M. Delaigue, P. Murphy and M. Fabretto, Flexible Polymer-on-Polymer Architecture for Piezo/Pyroelectric Energy Harvesting, *ACS Appl. Mater. Interfaces*, 2015, **7**, 8465–8471.

84 Y. Zi, L. Lin, J. Wang, S. Wang, J. Chen, X. Fan, P. K. Yang, F. Yi and Z. L. Wang, Triboelectric-pyroelectric-piezoelectric hybrid cell for high-efficiency energy-harvesting and self-powered sensing, *Adv. Mater.*, 2015, **27**, 2340–2347.

85 D. Kraemer, B. Poudel, H. P. Feng, J. C. Caylor, B. Yu, X. Yan, Y. Ma, X. Wang, D. Wang, A. Muto, K. McEnaney, M. Chiesa, Z. Ren and G. Chen, High-performance flat-panel solar thermoelectric generators with high thermal concentration, *Nature materials*, 2011, **10**, 532–538.

86 D. Beretta, N. Neophytou, J. M. Hodges, M. G. Kanatzidis, D. Narducci, M. Martin-Gonzalez, M. Beekman, B. Balke, G. Cerretti, W. Tremel, A. Zevalkink, A. I. Hofmann, C. Müller, B. Dörling, M. Campoy-Quiles and M. Caironi, Thermoelectrics: From history, a window to the future, *Mater. Sci. Eng. R Rep.*, 2019, **138**, 100501.

87 L. L. Baranowski, G. J. Snyder and E. S. Toberer, Concentrated solar thermoelectric generators, *Energy Environ. Sci.*, 2012, **5**, 9055.

88 F. Kim, B. Kwon, Y. Eom, J. E. Lee, S. Park, S. Jo, S. H. Park, B.-S. Kim, H. J. Im, M. H. Lee, T. S. Min, K. T. Kim, H. G. Chae, W. P. King and J. S. Son, 3D printing of shape-conformable thermoelectric materials using all-inorganic Bi_2Te_3-based inks, *Nat. Energy*, 2018, **3**, 301–309.
89 K. Biswas, J. He, I. D. Blum, C. I. Wu, T. P. Hogan, D. N. Seidman, V. P. Dravid and M. G. Kanatzidis, High-performance bulk thermoelectrics with all-scale hierarchical architectures, *Nature*, 2012, **489**, 414–418.
90 D. Kraemer, Q. Jie, K. McEnaney, F. Cao, W. Liu, L. A. Weinstein, J. Loomis, Z. Ren and G. Chen, Concentrating solar thermoelectric generators with a peak efficiency of 7.4%, *Nat. Energy*, 2016, **1**, 16153.
91 O. Neumann, A. D. Neumann, S. Tian, C. Thibodeaux, S. Shubhankar, J. Müller, E. Silva, A. Alabastri, S. W. Bishnoi, P. Nordlander and N. J. Halas, Combining Solar Steam Processing and Solar Distillation for Fully Off-Grid Production of Cellulosic Bioethanol, *ACS Energy Lett.*, 2016, **2**, 8–13.
92 Y. Zhang, S. K. Ravi and S. C. Tan, Food-derived carbonaceous materials for solar desalination and thermo-electric power generation, *Nano Energy*, 2019, **65**, 104006.
93 M. F. Dupont, D. R. MacFarlane and J. M. Pringle, Thermo-electrochemical cells for waste heat harvesting – progress and perspectives, *Chem. Commun.*, 2017, **53**, 6288–6302.
94 R. Hu, B. A. Cola, N. Haram, J. N. Barisci, S. Lee, S. Stoughton, G. Wallace, C. Too, M. Thomas, A. Gestos, M. E. Cruz, J. P. Ferraris, A. A. Zakhidov and R. H. Baughman, Harvesting waste thermal energy using a carbon-nanotube-based thermo-electrochemical cell, *Nano Lett.*, 2010, **10**, 838–846.
95 S. W. Lee, Y. Yang, H. W. Lee, H. Ghasemi, D. Kraemer, G. Chen and Y. Cui, An electrochemical system for efficiently harvesting low-grade heat energy, *Nat. Commun.*, 2014, **5**, 3942.
96 P. Yang, K. Liu, Q. Chen, X. Mo, Y. Zhou, S. Li, G. Feng and J. Zhou, Wearable Thermocells Based on Gel Electrolytes for the Utilization of Body Heat, *Angew. Chem.*, 2016, **55**, 12050–12053.
97 H. Im, T. Kim, H. Song, J. Choi, J. S. Park, R. Ovalle-Robles, H. D. Yang, K. D. Kihm, R. H. Baughman, H. H. Lee, T. J. Kang and Y. H. Kim, High-efficiency electrochemical thermal energy harvester using carbon nanotube aerogel sheet electrodes, *Nat. Commun.*, 2016, **7**, 10600.
98 M. S. Romano, N. Li, D. Antiohos, J. M. Razal, A. Nattestad, S. Beirne, S. Fang, Y. Chen, R. Jalili, G. G. Wallace, R. Baughman and J. Chen, Carbon nanotube - reduced graphene oxide composites for thermal energy harvesting applications, *Adv. Mater.*, 2013, **25**, 6602–6606.
99 A. Siria, M. L. Bocquet and L. Bocquet, New avenues for the large-scale harvesting of blue energy, *Nat. Rev. Chem.*, 2017, **1**, 0091.
100 F. La Mantia, M. Pasta, H. D. Deshazer, B. E. Logan and Y. Cui, Batteries for efficient energy extraction from a water salinity difference, *Nano Lett.*, 2011, **11**, 1810–1813.
101 Z. Jia, B. Wang, S. Song and Y. Fan, Blue energy: Current technologies for sustainable power generation from water salinity gradient, *Renewable Sustainable Energy Rev.*, 2014, **31**, 91–100.
102 J. W. Post, H. V. M. Hamelers and C. J. N. Buisman, Energy Recovery from Controlled Mixing Salt and Fresh Water with a Reverse Electrodialysis System, *Environ. Sci. Technol.*, 2008, **42**, 5785–5790.
103 A. P. Straub, A. Deshmukh and M. Elimelech, Pressure-retarded osmosis for power generation from salinity gradients: is it viable?, *Energy Environ. Sci.*, 2016, **9**, 31–48.
104 M. Simoncelli, N. Ganfoud, A. Sene, M. Haefele, B. Daffos, P. L. Taberna, M. Salanne, P. Simon and B. Rotenberg, Blue Energy and Desalination with Nanoporous Carbon Electrodes: Capacitance from Molecular Simulations to Continuous Models, *Phys. Rev. X*, 2018, **8**, 021024.
105 A. B. Pouyfaucon and L. García-Rodríguez, Solar thermal-powered desalination: A viable solution for a potential market, *Desalination*, 2018, **435**, 60–69.
106 E. Chiavazzo, M. Morciano, F. Viglino, M. Fasano and P. Asinari, Passive solar high-yield seawater desalination by modular and low-cost distillation, *Nature Sustainability*, 2018, **1**, 763–772.
107 T. Ding, K. Liu, J. Li, G. Xue, Q. Chen, L. Huang, B. Hu and J. Zhou, All-Printed Porous Carbon Film for Electricity Generation from Evaporation-Driven Water Flow, *Adv. Funct. Mater.*, 2017, **27**, 1700551.
108 J. Li, K. Liu, T. Ding, P. Yang, J. Duan and J. Zhou, Surface functional modification boosts the output of an evaporation-driven water flow nanogenerator, *Nano Energy*, 2019, **58**, 797–802.
109 J. Li, S. Gao, R. Long, W. Liu and Z. Liu, Self-pumped evaporation for ultra-fast water desalination and power generation, *Nano Energy*, 2019, **65**, 104059.
110 D. Perrone, J. Murphy and G. M. Hornberger, Gaining perspective on the water-energy nexus at the community scale, *Environ. Sci. Technol.*, 2011, **45**, 4228–4234.
111 J. Chen, J. Yang, Z. Li, X. Fan, Y. Zi, Q. Jing, H. Guo, Z. Wen, K. C. Pradel, S. Niu and Z. L. Wang, Networks of triboelectric nanogenerators for harvesting water wave energy: a potential approach toward blue energy, *ACS Nano*, 2015, **9**, 3324–3331.
112 J. Yin, Z. Zhang, X. Li, J. Yu, J. Zhou, Y. Chen and W. Guo, Waving potential in graphene, *Nat. Commun.*, 2014, **5**, 3582.
113 W. Wang, Y. Shi, C. Zhang, S. Hong, L. Shi, J. Chang, R. Li, Y. Jin, C. Ong, S. Zhuo and P. Wang, Simultaneous production of fresh water and electricity via multistage solar photovoltaic membrane distillation, *Nat. Commun.*, 2019, **10**, 3012.
114 B. Coelho, A. C. Oliveira and A. Mendes, Concentrated solar power for renewable electricity and hydrogen production from water-a review, *Energy Environ. Sci.*, 2010, **3**, 1398.
115 P. Tao, C. Chang, Z. Tong, H. Bao, C. Song, J. Wu, W. Shang and T. Deng, Magnetically-accelerated large-capacity solar-thermal energy storage within high-temperature phase-change materials, *Energy Environ. Sci.*, 2019, **12**, 1613–1621.

116 A. V. Dudchenko, C. Chen, A. Cardenas, J. Rolf and D. Jassby, Frequency-dependent stability of CNT Joule heaters in ionizable media and desalination processes, *Nat. Nanotechnol.*, 2017, **12**, 557–563.

117 J. Huang, Y. He, Y. Hu and X. Wang, Coupled photothermal and joule-heating process for stable and efficient interfacial evaporation, *Sol. Energy Mater. Sol. Cells*, 2019, **203**, 110156.

118 P. Behnam and M. B. Shafii, Examination of a solar desalination system equipped with an air bubble column humidifier, evacuated tube collectors and thermosyphon heat pipes, *Desalination*, 2016, **397**, 30–37.

119 M. Howells and H. H. Rogner, Water-Energy Nexus Assessing integrated systems, *Nat. Clim. Change*, 2014, **4**, 246–247.

120 A. M. Hamiche, A. B. Stambouli and S. Flazi, A review of the water-energy nexus, *Renewable Sustainable Energy Rev.*, 2016, **65**, 319–331.

121 J. Harold James Willard, Synergy City a production facility for electrical power, fresh water, and trash processing without the use of nuclear fission, coal or oil, *US Pat.*, US2011/0266207 A1, 2011.